Measurement of the Polarized Forward-Backward Asymmetry of $Z^0 \to b\bar{b}$ Using a Mass Tag and Momentum-Weighted Track Charge

The SLD Collaboration [1]

Stanford Linear Accelerator Center
Stanford University
Stanford, CA 94309

ABSTRACT

We present a direct measurement of the parity-violating parameter A_b by analyzing the left-right forward-backward asymmetry of b quarks in $e^+e^- \to Z^0 \to b\bar{b}$. The SLD experiment observes hadronic decays of Z^0 bosons produced at resonance in collisions of longitudinally polarized electrons and unpolarized positrons at the SLC. Heavy flavor decays of the Z^0 are identified by using the topologically reconstructed mass of B hadrons. The asymmetry A_b is measured with a self-calibrating technique employing momentum-weighted track charge from both hemispheres in the tagged events. From our 1994–1995 sample of 3.6 pb^{-1} of e^+e^- annihilation data with a luminosity-weighted average e^- polarization of 77%, and our 1993 sample of 1.8 pb^{-1} with a luminosity-weighted polarization of 63%, we obtain $A_b = 0.911 \pm 0.045(\text{stat.}) \pm 0.045(\text{syst.})$.

---

1   Introduction

Measurements of fermion production asymmetries at the Z^0 pole provide probes of the combination of vector (v) and axial vector (a) couplings $A_f = 2v_f a_f/(v_f^2 + a_f^2)$, which express the extent of parity violation in the Zff coupling. At Born level, the Z^0 peak differential cross section for producing a final state fermion f at an angle $z = \cos\theta$ from the electron beam direction is

$$\sigma^f(z) \equiv d\sigma_f/dz \propto (1 - A_e P_e)(1 + z^2) + 2A_f(A_e - P_e)z, \qquad (1)$$

where P_e is the longitudinal polarization of the electron beam. By manipulating the sign of P_e, it is possible to measure the left-right forward-backward asymmetry for b quark production [1]

$$\tilde{A}_{FB}^b(z) = \frac{[\sigma_L^b(z) - \sigma_L^b(-z)] - [\sigma_R^b(z) - \sigma_R^b(-z)]}{\sigma_L^b(z) + \sigma_L^b(-z) + \sigma_R^b(z) + \sigma_R^b(-z)} = |P_e|A_b\frac{2z}{1 + z^2}, \qquad (2)$$

where L, R refers to $Z^0 \to b\bar{b}$ decays produced with a predominantly left-handed (negative helicity) or right-handed (positive helicity) electron beam, respectively. The measurement of the double asymmetry eliminates the dependence on the Zee coupling parameter A_e. The quantity A_b is largely independent of propagator effects that modify the effective weak mixing angle ($\delta A_b = -0.63 \cdot \delta \sin^2\theta_W^{\text{eff}}$), and thus is complementary to other electroweak asymmetry measurements performed at the Z^0 pole.

In this paper we present a measurement of $\tilde{A}_{FB}^b(z)$ from $93 - 95$ data using an inclusive vertex mass tag to select an enriched sample of $Z^0 \to b\bar{b}$ events, and the net momentum-weighted track charge, first suggested by Feynman and Field [2], to identify the sign of the charge of the underlying b quark. This technique was pioneered at lower energies [3], and more recently applied at the Z^0 in conjunction with a lifetime tag [4][5][6]. The first direct measurements of the extent of parity violation in the Zbb coupling were made by SLD using momentum-weighted track charge [7] and leptons from semileptonic B hadron decay [8]. The analysis presented in this paper is based on momentum-weighted track charge with an improved calibration technique which greatly reduces model dependence.

The operation of the SLAC Linear Collider (SLC) with a polarized electron beam has been described previously [9]. During the 1993 running period, the SLC Large Detector (SLD) recorded 1.8 pb^{-1} of e^+e^- annihilation data at a mean center-of-mass energy of 91.26 ± 0.02 GeV, with a mean electron beam longitudinal polarization of $(63 \pm 1)\%$. In 1994–1995, SLD recorded 3.6 pb^{-1} at the same energy, but with a mean longitudinal polarization of $(77.2 \pm 0.5)\%$. Charged particles were tracked in the Central Drift Chamber (CDC) [10] in a uniform axial magnetic field of 0.6T. In addition, a pixel-based CCD vertex detector (VXD) [11] provides an accurate measure of particle trajectories close to the beam axis. The momentum resolution of the combined CDC and VXD systems is $(\delta p_\perp/p_\perp)^2 = (.01)^2 + (.0026p_\perp)^2$, where $p_\perp$ is the momentum in GeV/c perpendicular to the beamline. The thrust axis [12] was reconstructed using the Liquid Argon Calorimeter [13], which covers a range of $|\cos\theta| < 0.98$.

The luminous region of the SLC interaction point (IP) has a size of about $(1.5 \times 0.8 \times 700)$ μm in (x,y,z). We use the average $\langle IP \rangle$ position of sequential hadronic events to determine the primary vertex (PV) in $r\phi$, the plane transverse to the beam direction. The longitudinal position of the PV is determined for each event individually [14]. This results in a PV with uncertainties of 7 μm transverse to the beam axis and 35 μm (52 μm for $b\bar{b}$ events) along it. The measured track impact parameter resolution is $\sigma_{r\phi}[\mu m] = 11 \oplus 70/p\sin^{3/2}\theta$, $\sigma_{rz}[\mu m] = 37 \oplus 70/p\sin^{3/2}\theta$ where p is the track momentum expressed in GeV/c.

2   Event Selection and Momentum-Weighted Track Charge

For the purpose of selecting hadronic events and calculating the momentum-weighted track charge, a loose set of requirements was placed on reconstructed tracks, while stricter requirements were placed on tracks used to select $Z^0 \rightarrow b\bar{b}$ candidates. "Track-charge quality" tracks were required to have: i) $p_\perp \geq 0.15$ GeV/c and $p_{tot} < 50$ GeV/c; ii) $|\cos\theta| \leq 0.8$; and iii) point of closest approach to the beam line within a cylinder of radius r_0 and half-length l_0 about the IP of $(r_0, l_0) = (2.0, 10.0)$ cm; and iv) not been identified as a decay product of a Λ, K_s^0, or γ-conversion. "Tag quality" tracks were additionally required to have: i) the point of closest approach within $(r_0, l_0) = (0.3, 1.5)$ cm; ii) at least one VXD hit; and iii) XY impact parameter resolution $\sigma_d < 250\mu m$.

Events were classified as hadronic decays of the Z^0 provided that they contained at least 7 track-charge quality tracks, a visible charged energy of at least 20 GeV, and a thrust axis satisfying $|\cos\theta_{thrust}| < 0.7$. The resulting hadronic sample from $93 - 95$ data contained 76554 events with $< 0.1\%$ non-hadronic background.

From this hadronic sample, two and three jet events were selected using the JADE jet-finding algorithm [15] with the parameter $y_{cut} = 0.02$, leaving 71951 events in the sample.

To enrich the sample with $Z^0 \rightarrow b\bar{b}$ events, a b tag based on topological reconstruction of B-decay vertices was applied. The ZVTOP program [16] was used for secondary vertex finding with tag quality tracks as input. For a hemisphere where a secondary vertex was found, more tracks were attached to the seed secondary vertex on the basis of the longitudinal ($L/D > 0.25$) and transverse ($T < 1$ mm) distance from the vertex. See Figure 1 for a definition of the variables D, L and T. Each track was assigned a pion mass and correction for missing transverse momentum was applied to account for neutral particles. After that, the mass of the B hadron candidate was calculated. More information on the SLD mass tag performance can be found in [17].

The vertex mass distribution calculated for the data and Monte Carlo is shown in Figure 2. As can be seen from this picture, the $Z^0 \rightarrow c\bar{c}$ event contribution has a clear cut-off at $1.8 - 2.0$ GeV. This feature makes the mass tag very attractive for measurements requiring high-purity b tag.
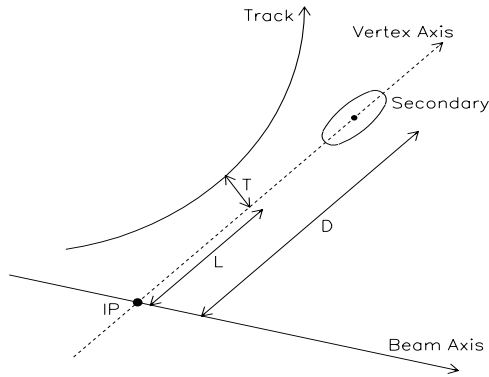
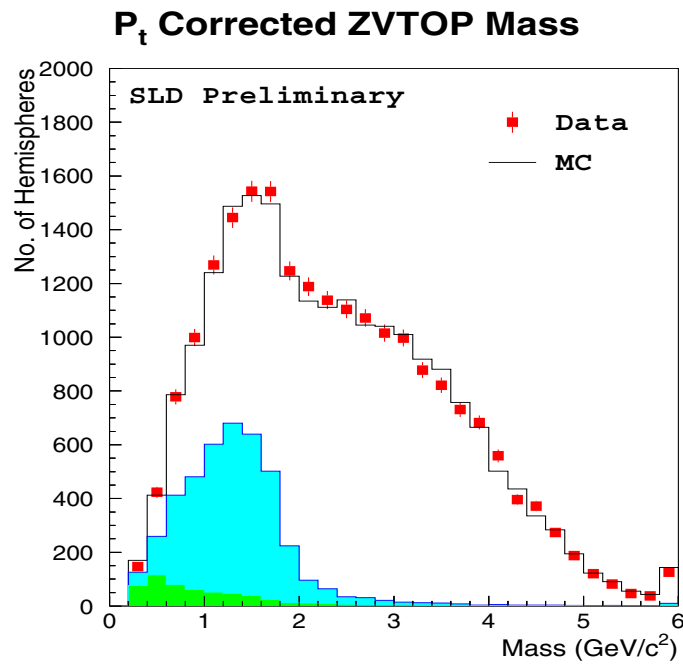Figure 1: Parameters used to assign a track to the seed vertex: $T < 1$ mm, $L/D > 0.25$.

Figure 2: Mass distribution for data and Monte Carlo. The dark shaded area under the histogram represents the contribution from uds and the light shaded area from c quarks. The unshaded region is due to b quarks.
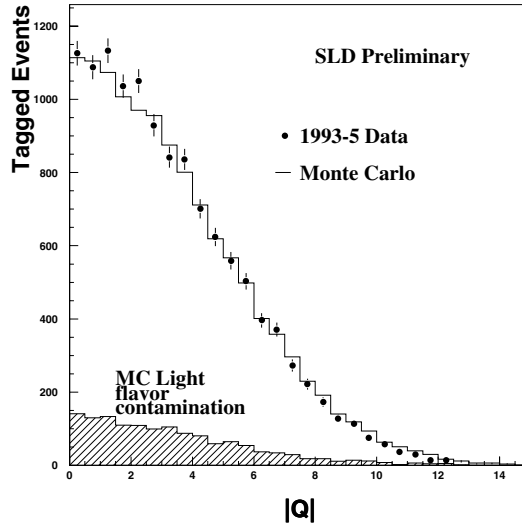
Figure 3: Comparison of the momentum-weighted charge $|Q|$ between data and Monte Carlo

The maximum of masses from the two hemispheres in the event was used as a tag variable in this analysis:

$$MASS = MAX(mass1, mass2) . \tag{3}$$

For the current measurement we required $MASS > 1.6~GeV$. This selection is 65% efficient for identifying $Z^0 \rightarrow b\bar{b}$ events, with a purity of 91%. A total of 11092 events were selected.

Using all track-charge quality tracks, we formed the event momentum-weighted charge sum [2]

$$Q = - \sum_{tracks} q_i \cdot \text{sgn}(\vec{p}_i \cdot \hat{T})|(\vec{p}_i \cdot \hat{T})|^\kappa, \tag{4}$$

as well as the hemisphere summed momentum-weighted charge

$$Q_s = \sum_{tracks} q_i |(\vec{p}_i \cdot \hat{T})|^\kappa, \tag{5}$$

where q_i and $\vec{p}_i$ are the track charge and momentum, and $\hat{T}$ is the unit vector in the direction of the reconstructed thrust axis, signed so that $Q > 0$, making $\hat{T}$ an estimate of the b quark direction. We have chosen $\kappa = 0.5$ to maximize the analyzing power (AP) of the track charge algorithm for $Z^0 \rightarrow b\bar{b}$ events

$$AP = \frac{P_{cor} - P_{inc}}{P_{cor} + P_{inc}} \simeq 38\%, \tag{6}$$

where P_{cor} (P_{inc}) is the probability of assigning the b quark to the correct (incorrect) thrust hemisphere. Figure 3 shows a comparison of the Q distribution between data and MC. Figure 4 shows the $\hat{T}_z$ distribution for the enriched sample separately for left- and right-handed electron beam.
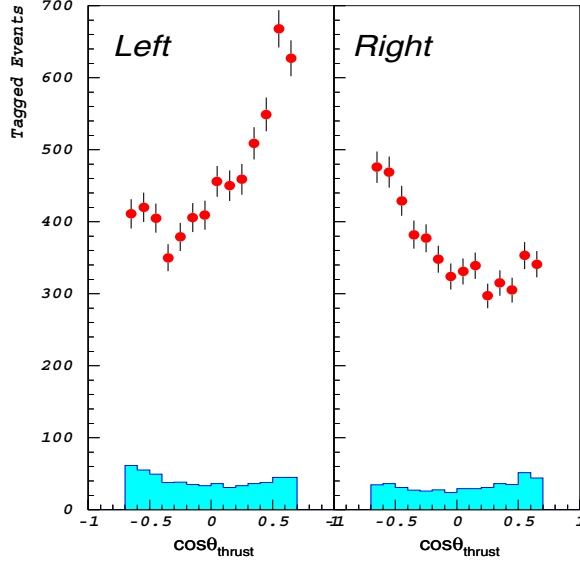
5

Figure 4: Distribution of $\cos\theta$ for the signed thrust axis in the 1993-1995 tagged sample. A clear forward-backward asymmetry is observed, with sign as expected from the cross section formula in Equation 1. Monte Carlo – estimated background is shown by the shaded region.

3 Maximum-Likelihood Analysis

The technique used to extract A_b from the data is a self-calibrated Maximum-Likelihood analysis, which takes advantage of the fact that the two hemispheres of a tagged event provide separate momentum-weighted track charges, which provide nearly independent information about the direction of the b quark. The likelihood function chosen for this analysis is based on the differential cross-section (see Equation 1):

$$ln\mathcal{L} = \sum_{events} ln\left(\rho(event_i, A_b, A_c)\right), \tag{7}$$

with

$$\begin{aligned} \rho(event_i, A_b, A_c) = (1 - A_e P_e^i)(1 + \cos^2\theta_i) + 2(A_e - P_e^i)\cos\theta_i[\\ A_b f_i^b (2p_i^{correct,b} - 1)(1 - \Delta_{QCD,b}^i) + \\ A_c f_i^c (2p_i^{correct,c} - 1)(1 - \Delta_{QCD,c}^i) + \\ A_{bckg}(1 - f_i^b - f_i^c)(2p_i^{"correct",bckg} - 1)], \tag{8} \end{aligned}$$

where A_e is the asymmetry in electron coupling to the Z^0, P_e^i is the signed polarization of the electron beam when that event was recorded, $f_i^{b(c)}$ are the probabilities that that event was a $Z^0 \to b\bar{b}(c\bar{c})$ decay, and are parameterized as a function of the secondary vertex mass, and $\Delta_{QCD,b,c}^i$ are final-state QCD corrections, to be discussed in Sections 3.3, 3.4 and 4. A_{bckg} is an estimated asymmetry from $u\bar{u}$, $d\bar{d}$, and $s\bar{s}$ decays of the Z^0. The correct-sign probabilities $p^{correct,b}$ and $p^{correct,c}$ are estimated as functions

6

of the momentum weighted charge $|Q|$, defined in Equation 4. The $p^{correct,b,c}(|Q|)$ parameterize how well the algorithm signs the thrust axis and may be estimated from the Monte Carlo, but $p^{correct,b}$ can be inferred from the data with a much reduced model dependence (see Section 3.1).

While A_e appears in the likelihood function of Equation 8, the dependence of the fitted A_b on the assumed value of A_e is very small and must vanish in the limit of large statistics. This can be seen by dividing Equation 8 by $(1 - A_e P_e^i)$, which does not affect the fit. If the data is then analyzed with $P_e^i = \pm 1$, retaining only the sign of the polarization in each event, then the likelihood function would be manifestly independent of A_e. The value of A_b would then be extracted by dividing the resulting fit value by the luminosity-weighted average polarization $\langle P_e \rangle_{\mathcal{L}}$. The only differences in the fit results arising from using an event-by-event polarization or dividing by a luminosity-weighted polarization after the fit are statistical in nature.

3.1 Calibrating the Analyzing Power

The functional form of $p^{correct,b}(|Q|)$ can be derived with the aid of two assumptions about the hemisphere momentum-weighted charge distributions. These assumptions are that the momentum-weighted charge in the b hemisphere, Q_b, and the momentum-weighted charge in the $\bar{b}$ hemisphere, $Q_{\bar{b}}$, are Gaussian and uncorrelated. The effect of interhemisphere correlation will be incorporated in Section 3.2.

With these assumptions, a calibration procedure for the correct-sign probability using the momentum-weighted charges in the two hemispheres may be formulated. The quantities

$$Q_{sum} = Q_b + Q_{\bar{b}} \tag{9}$$

and

$$Q_{dif} = Q_b - Q_{\bar{b}} \tag{10}$$

are identifiable with observable variables: $Q_{sum} = Q_s$, and $|Q_{dif}| = |Q|$, defined in Equations 5 and 4. The correct-sign probability $p^{correct,b}(|Q|)$ is the fraction the time $Q_{dif} < 0$ when $|Q_{dif}| = |Q|$. The task is to find the mean q_0 and width σ of the Gaussian Q_{dif} distribution. With these in hand,

$$p^{correct,b}(|Q|) = \frac{1}{1 + e^{-\alpha_b |Q|}} \ , \tag{11}$$

with

$$\alpha_b = 2q_0/\sigma^2. \tag{12}$$

These two variables can be easily obtained from the data:

$$\sigma^2 = \sigma_{sum}^2 = \sigma_{dif}^2 = \langle |Q_{dif}|^2 \rangle - (q_0)^2, \tag{13}$$

and

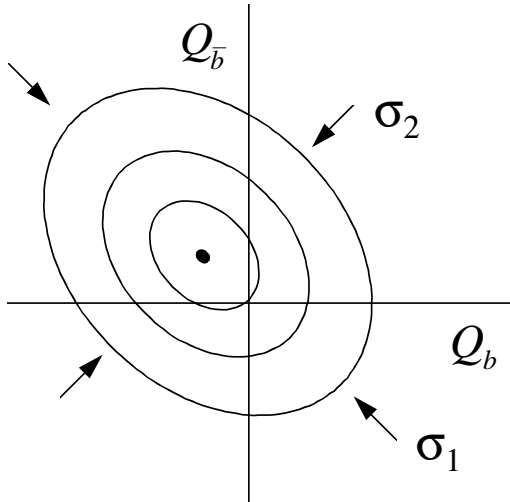$$q_0 = \sqrt{\langle |Q_{dif}|^2 \rangle - \sigma_{sum}^2} \ . \tag{14}$$

Figure 5: Effect of inter-hemisphere correlations on the momentum-weighted charge distributions.

3.2 Interhemisphere Correlation

While this calibration of the correct-sign probability accounts for nearly all of the charge-diluting effects present in the data, a departure from the uncorrelated probability assumption produces a shift in the α_b derived in the last section. This correlation arises because of the nature of the hadronization process, which demands total charge conservation in the event, and tracks which migrate from one thrust hemisphere to the other.

The effect of correlation is to distort the joint probability of Q_b and $Q_{\bar{b}}$ from a circular Gaussian distribution to a Gaussian ellipsoid, stretched along one of the 45° diagonals, shown in Figure 5. The effect is to change σ_{dif}, the width of the signed Q_{dif} distribution, relative to σ_{sum}, the width of the signed Q_{sum} distribution:

$$\sigma_{dif} = (1 + \lambda)\sigma_{sum} .\tag{15}$$

The uncorrelated hypothesis used the same value for these two, σ_{sum}. The correlation is incorporated into the analysis by using Equation 15 in the expression for α_b:

$$\alpha = \frac{2\sqrt{\langle|Q_{dif}|^2\rangle - (1 + \lambda)^2\sigma_{sum}^2}}{(1 + \lambda)^2\sigma_{sum}^2} .\tag{16}$$

The correlation λ has been estimated to be 2.7% using JETSET 7.4 [18] with parton shower evolution and string fragmentation, and full detector simulation.

3.3 QCD Corrections

Effects of the b-quark axis smearing due to the final state QCD radiation are incorporated in the analysis by applying a correction Δ_{QCD} to the maximum likelihood

function (Equation 8). Theoretical calculations of the QCD corrections to the asymmetry may be found in the literature [19] [20]. However, these calculations use the b-quark direction to define the asymmetry, whereas in this analysis the thrust axis of the event is used as an estimate of the initial quark direction. The thrust axis, taking into account the momentum flow of the whole event, is less sensitive to the QCD radiation. Theoretical estimates [21] [22] show that $\Delta_{QCD}^{Thrust} = (0.9 - 0.95)\Delta_{QCD}^{Quark}$ at the parton level. One has to note, however, that in the case of a three-particle final state ($q\bar{q}g$) the thrust axis is always parallel to the direction of flight of the particle with the highest momentum. Also the b-tagging procedure and momentum-weighted track-charge technique [5] used in this measurement suppress events with hard gluon radiation.

Consequently, we have taken a different approach. The first-order theoretical calculations by J.B.Stav and H.A.Olsen [20] for massive quarks were used as a basis:

$$\Delta_{SO}(|\cos\theta|) = 1 - \frac{A_q(|\cos\theta|)}{A_0} \ , \tag{17}$$

where A_0 is the Born-level asymmetry (Section 1) and A_q is the asymmetry based on the b-quark direction after all perturbative radiation. Then Δ_{SO} was corrected for the analysis bias (thrust axis, b-tag and Jet Charge). The total correction is then:

$$\Delta_{QCD} = 1 - \frac{A_{exp}}{A_0} = x\Delta_{SO} \ , \tag{18}$$

with x estimated from the Monte Carlo and defined as:

$$x = \frac{1 - \frac{A_{exp}}{A_0}}{1 - \frac{A_q}{A_0}} \ . \tag{19}$$

A_{exp} is the asymmetry measured in the experiment. The value $x = 0$ would mean that the measured A_b is not sensitive to gluon radiation and no QCD corrections need to be applied, while $x = 1$ would mean that there is no analysis bias so that the theoretical correction Δ_{SO} must be applied in full.

A generator-level Monte Carlo was used to estimate x. JETSET7.4 with the first order matrix element (parameter MSTJ(101)=1) was used to generate events. Then a simple model of detector acceptance, analysis and tag cuts was applied. The self-calibrating maximum likelihood method was used next to extract A_{exp} in each bin of $|\cos\theta|$. The average correction in the $|\cos\theta|$ range of $0 - 0.7$ was found to be: $x = 0.25 \pm 0.08$ with $\chi^2 = 1.4/dof$.

As a result, the total QCD correction applied in the analysis was:

$$\Delta_{QCD}(|\cos\theta|) = 0.25\Delta_{SO}(|\cos\theta|) \ . \tag{20}$$

The total QCD correction used in the analysis, Δ_{QCD}, as well as the theoretical calculations, Δ_{SO}, are shown in Figure 6.

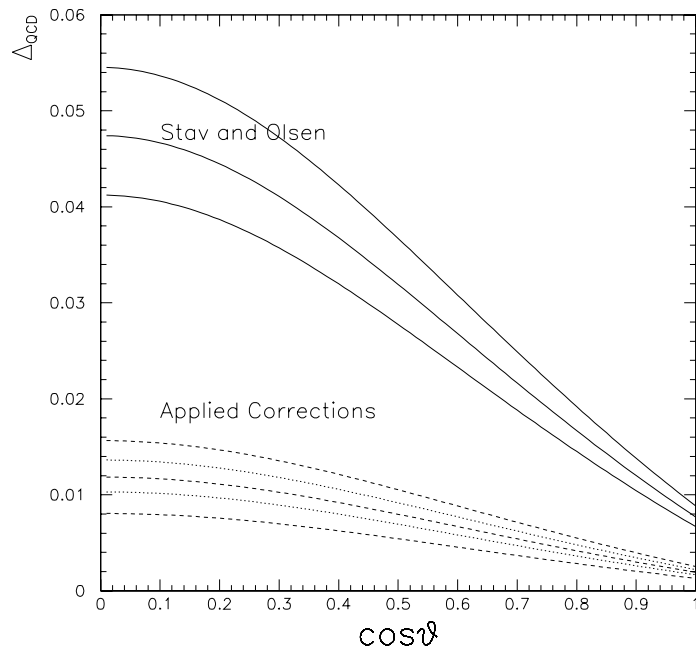Figure 6: Theoretical calculation by Stav and Olsen, Δ_{SO} (solid line), and total QCD correction applied in the analysis, Δ_{QCD} (dashed line). The solid line band represents the uncertainty in the theoretical calculation, mainly due to the error in α_s. The dashed line band corresponds to statistical errors in x, and the dotted line band covers the theoretical uncertainty in Δ_{QCD}.

Table 1: Calibration parameters for the data and Monte Carlo. Errors are statistical only.

	Data	Monte Carlo
σ_{sum}	3.755 ± 0.025	3.857 ± 0.010
$\sqrt{\langle |Q_{dif}|^2 \rangle}$	4.259 ± 0.028	4.383 ± 0.011
λ	assume same as MC	0.027
α_b	0.249 ± 0.013	0.245 ± 0.005

3.4 Measurement of A_b

To determine α_b, the data σ_{sum} and $\langle |Q_{dif}|^2 \rangle$ are corrected for light-flavor contamination in the tag, which modifies α_b by a small amount. The value of α_b is also allowed to vary as a function of $\cos\theta$, owing to the geometrical tracking acceptance, and so a Monte Carlo model of its dependence on polar angle is scaled to the overall α_b measured from tagged events in the data.

The $Zb\bar{b}$ event probability, f^b, is calculated from the data using a double tag technique [23]. Charm and bottom events production fractions, R_c and R_b, were used as input parameters. Tagging efficiencies for charm and uds events were estimated from the Monte Carlo.

The remaining ingredients to the likelihood function of Equation 8 are obtained from Monte Carlo: the charm probability f^c and $p^{correct,c}$. The value of A_c is set to its Standard Model value of 0.67, and the value of A_{bckg} is set to zero. The error arising from the latter is very small owing to its $\sim 1\%$ fraction in the tagged sample.

The value of A_b extracted from the fit and corrected for a small effect of the initial state radiation (0.17%) is $A_b = 0.911 \pm 0.045$ ($stat$).

4 Systematic Errors

Systematic errors arise from the use of Monte Carlo modeling in the likelihood fit, and the statistical power of the fit for α_b. The statistical error on σ_{sum} and $\sigma_{|Q_{dif}|}$ in the data will scale with $1/\sqrt{N}$. The validity of the Gaussian assumption for the shape of Q_b and $Q_{\bar{b}}$ was checked with a simulation that generated various triangular distributions as well as a double Gaussian with tails and offset mean, and only small deviations were seen in the measured A_b when the underlying shape was modified. The shape of Q_{sum} in the data constrains the shape of $p(Q_b)$ to be close to Gaussian. Because $|Q_b|$ and $|Q_{\bar{b}}|$ share the same probability distribution, that distribution is observable in the data and may also be used to provide tighter constraints on the Gaussian shape hypothesis. No deviations from the Gaussian hypothesis were seen, and the trial functions were ruled out with high confidence.

Table 2: Summary of λ_b systematic error analysis.

Parameter		Nominal Value	Variation	$\delta\lambda_{b, \ gen}$ (%)
Λ_{QCD},	PARJ(81)	0.26	$0.24 - 0.28$	0.06 ± 0.14
Q_0,	PARJ(82)	1.0	$0.7 - 1.8$	0.17 ± 0.14
σ_q,	PARJ(21)	0.37	$0.32 - 0.40$	0.20 ± 0.14
γ_s,	PARJ(2)	0.28	$0.25 - 0.32$	0.19 ± 0.14
$[V/(V + S)]_{u,d}$,	PARJ(11)	0.50	$0.30 - 0.75$	0.27 ± 0.14
$[V/(V + S)]_s$,	PARJ(12)	0.45	$0.45 - 0.60$	0.11 ± 0.14
$[V/(V + S)]_{c,b}$,	PARJ(13)	0.53	$0.53 - 0.63$	0.05 ± 0.14
ϵ_b,	PARJ(55)	0.006	$0.006 - 0.0277$	0.04 ± 0.14
direct baryon rate,	PARJ(1)	0.08	$0.08 - 0.12$	0.20 ± 0.14
popcorn parameter,	PARJ(5)	1.	$0. - 2.$	0.11 ± 0.14
x_d,	PARJ(76)	0.7	$0. - 0.7$	0.16 ± 0.14
x_s,	PARJ(77)	10.	$0. - 100.$	0.18 ± 0.14
HERWIG5.7				0.29 ± 0.11
Total				0.6%

One of the largest errors in the analysis involves the estimation of the inter-hemisphere correlation. The value of the correlation between hemispheres was obtained from the Monte Carlo: $\lambda_b = 2.67 \pm 0.11\%(stat)$. The systematic uncertainty was estimated by varying the JETSET7.4 model parameters and comparing to a Monte Carlo model with a completely different fragmentation scheme – HERWIG5.7 . Since we do not have any samples of fully reconstructed HERWIG5.7 or JETSET7.4 with altered parameters, the study was done at the generator level. The Monte Carlo was allowed to decay unstable particles, and a simple model of detector acceptance, tag and analysis cuts was applied. Then generator–level correlations were calculated. In order to obtain the value of λ_b at the reconstructed level, generator–level correlations were scaled down with a ratio of

$$\frac{\lambda_{full}^{JETSET}}{\lambda_{generator}^{JETSET}} = 0.61 \ , \qquad (21)$$

where λ_{full}^{JETSET} is the correlation extracted from the fully reconstructed tuned JETSET7.4 Monte Carlo model, and $\lambda_{generator}^{JETSET}$ is the correlation with the generator-level tuned JETSET7.4. Table 2 shows the Monte Carlo model parameters that were changed, and the range of variations and resulting changes in the correlation at the generator level. The total uncertainty in the reconstructed level correlation was taken to be

$$\sigma_{\lambda_b} = 0.4\% \ . \qquad (22)$$

Different models were chosen for the $\cos\theta$ dependence of the α_b shape, but since the overall scale is determined by that in the data, the effect on the measured A_b is small.

The models of the sum and difference widths of the tagged u, d, s, and c events

are close to the observed b sum and difference widths, so the correction to α_b from their presence in the tag is small.

The dominant model errors come from estimations of the tag purity. The resulting purity of the tagged data sample with the selected mass cut of 1.6 GeV/c^2 is $\Pi_b = 91.11 \pm 0.91\%$ where systematic uncertainties in the charm-tag efficiency (ϵ_c) and charm production (R_c) are the main contributions to the error. Uncertainties in ϵ_c, ϵ_{uds} are estimated similar to the Ref. [17]. This error will decrease with a larger data sample.

Discrepancies in tracking efficiency and resolution between the data and Monte Carlo can affect the measured value of A_b. In the simulation track Z impact parameters were smeared using a random Gaussian distribution of width 20 μm/$\sin\theta$ to match the data. The difference between the simulated and measured charged track multiplicity of 0.5 track/event was attributed to an unsimulated tracking inefficiency corrections. To calculate the final value of A_b, corrections were applied to the Monte Carlo events for tracking efficiency and smearing of the track impact parameter. The total change in measured A_b, with and without smearing, was taken as the systematic error: $\delta A_b/A_b = 0.6\%$. Also, effects of the tracking efficiency corrections on the tag and jet charge were studied separately, resulting in an additional relative 1.4% uncertainty.

The error on the QCD correction includes statistical and systematic error in analysis bias x, second order effects, theoretical uncertainty in Δ_{SO} calculations, and a full range of QCD corrections for $Zc\bar{c}$ events.

The combined 1993-1995 SLD measurement of A_b using momentum-weighted track charge is

$$A_b(\text{Preliminary}) = 0.911 \pm 0.045(\text{stat.}) \pm 0.045(\text{syst.}), \qquad (23)$$

consistent with the Standard Model prediction of 0.935.

5   Acknowledgments

Table 3: Relative systematic errors on the measurement of A_b.

Error Source	Variation	$\delta A_b / A_b$
Self-Calibration		
α_b statistics	1σ	3.7%
Hemisphere Correlation	JETSET, HERWIG	1.7%
$P(Q_b)$ shape	Triangular, other shapes	0.8%
$\cos\theta$ shape of α_b	MC Shape *vs* Flat	0.4%
Light Flavor Subtraction	50% of correction	0.4%
Analysis		
Tag Composition	Mostly ϵ_c	1.5%
Detector Modeling	Efficiency Corrections, Smearing	1.5%
Beam Polarization	0.8%	0.8%
QCD	x, 2nd order terms, $\alpha_s \pm 0.007$	0.6%
A_c	0.67 ± 0.08	0.8%
A_{bckg}	0 ± 0.50	0.1%
A_e	0.1506 ± 0.00282	$\ll 0.1\%$
Gluon Splitting	100%	0.2%
Total		**4.9%**

The SLD Collaboration

K. Abe,[19] K. Abe,[30] T. Akagi,[28] N.J. Allen,[4] W.W. Ash,[28]† D. Aston,[28]
K.G. Baird,[24] C. Baltay,[34] H.R. Band,[33] M.B. Barakat,[34] G. Baranko,[9]
O. Bardon,[15] T. L. Barklow,[28] G.L. Bashindzhagyan,[18] A.O. Bazarko,[10]
R. Ben-David,[34] A.C. Benvenuti,[2] G.M. Bilei,[22] D. Bisello,[21] G. Blaylock,[16]
J.R. Bogart,[28] B. Bolen,[17] T. Bolton,[10] G.R. Bower,[28] J.E. Brau,[20]
M. Breidenbach,[28] W.M. Bugg,[29] D. Burke,[28] T.H. Burnett,[32]
P.N. Burrows,[15] W. Busza,[15] A. Calcaterra,[12] D.O. Caldwell,[5] D. Calloway,[28]
B. Camanzi,[11] M. Carpinelli,[23] R. Cassell,[28] R. Castaldi,[23](a) A. Castro,[21]
M. Cavalli-Sforza,[6] A. Chou,[28] E. Church,[32] H.O. Cohn,[29] J.A. Coller,[3]
V. Cook,[32] R. Cotton,[4] R.F. Cowan,[15] D.G. Coyne,[6] G. Crawford,[28]
A. D'Oliveira,[7] C.J.S. Damerell,[25] M. Daoudi,[28] N. de Groot,[28]
R. De Sangro,[12] R. Dell'Orso,[23] P.J. Dervan,[4] M. Dima,[8] D.N. Dong,[15]
P.Y.C. Du,[29] R. Dubois,[28] B.I. Eisenstein,[13] R. Elia,[28] E. Etzion,[33]
S. Fahey,[9] D. Falciai,[22] C. Fan,[9] J.P. Fernandez,[6] M.J. Fero,[15] R. Frey,[20]
T. Gillman,[25] G. Gladding,[13] S. Gonzalez,[15] E.L. Hart,[29] J.L. Harton,[8]
A. Hasan,[4] Y. Hasegawa,[30] K. Hasuko,[30] S. J. Hedges,[3] S.S. Hertzbach,[16]
M.D. Hildreth,[28] J. Huber,[20] M.E. Huffer,[28] E.W. Hughes,[28] H. Hwang,[20]
Y. Iwasaki,[30] D.J. Jackson,[25] P. Jacques,[24] J. A. Jaros,[28] Z. Y. Jiang,[28]
A.S. Johnson,[3] J.R. Johnson,[33] R.A. Johnson,[7] T. Junk,[28] R. Kajikawa,[19]
M. Kalelkar,[24] H. J. Kang,[26] I. Karliner,[13] H. Kawahara,[28] H.W. Kendall,[15]
Y. D. Kim,[26] M.E. King,[28] R. King,[28] R.R. Kofler,[16] N.M. Krishna,[9]
R.S. Kroeger,[17] J.F. Labs,[28] M. Langston,[20] A. Lath,[15] J.A. Lauber,[9]
D.W.G.S. Leith,[28] V. Lia,[15] M.X. Liu,[34] X. Liu,[6] M. Loreti,[21] A. Lu,[5]
H.L. Lynch,[28] J. Ma,[32] G. Mancinelli,[24] S. Manly,[34] G. Mantovani,[22]
T.W. Markiewicz,[28] T. Maruyama,[28] H. Masuda,[28] E. Mazzucato,[11]
A.K. McKemey,[4] B.T. Meadows,[7] R. Messner,[28] P.M. Mockett,[32]
K.C. Moffeit,[28] T.B. Moore,[34] D. Muller,[28] T. Nagamine,[28] S. Narita,[30]
U. Nauenberg,[9] H. Neal,[28] M. Nussbaum,[7]† Y. Ohnishi,[19] N. Oishi,[19]
D. Onoprienko,[29] L.S. Osborne,[15] R.S. Panvini,[31] C.H. Park,[27] H. Park,[20]
T.J. Pavel,[28] I. Peruzzi,[12](b) M. Piccolo,[12] L. Piemontese,[11] E. Pieroni,[23]
K.T. Pitts,[20] R.J. Plano,[24] R. Prepost,[33] C.Y. Prescott,[28] G.D. Punkar,[28]
J. Quigley,[15] B.N. Ratcliff,[28] T.W. Reeves,[31] J. Reidy,[17] P.L. Reinertsen,[6]
P.E. Rensing,[28] L.S. Rochester,[28] P.C. Rowson,[10] J.J. Russell,[28]
O.H. Saxton,[28] T. Schalk,[6] R.H. Schindler,[28] B.A. Schumm,[6] J. Schwiening,[28]
S. Sen,[34] V.V. Serbo,[33] M.H. Shaevitz,[10] J.T. Shank,[3] G. Shapiro,[14]
D.J. Sherden,[28] K.D. Shmakov,[29] C. Simopoulos,[28] N.B. Sinev,[20]
S.R. Smith,[28] M.B. Smy,[8] J.A. Snyder,[34] H. Staengle,[8] P. Stamer,[24]
H. Steiner,[14] R. Steiner,[1] M.G. Strauss,[16] D. Su,[28] F. Suekane,[30]
A. Sugiyama,[19] S. Suzuki,[19] M. Swartz,[28] A. Szumilo,[32] T. Takahashi,[28]
F.E. Taylor,[15] E. Torrence,[15] A.I. Trandafir,[16] J.D. Turk,[34] T. Usher,[28]
J. Va'vra,[28] C. Vannini,[23] E. Vella,[28] J.P. Venuti,[31] R. Verdier,[15]
P.G. Verdini,[23] D.L. Wagner,[9] S.R. Wagner,[28] A.P. Waite,[28] S.J. Watts,[4]
A.W. Weidemann,[29] E.R. Weiss,[32] J.S. Whitaker,[3] S.L. White,[29]
F.J. Wickens,[25] D.C. Williams,[15] S.H. Williams,[28] S. Willocq,[28] R.J. Wilson,[8]
W.J. Wisniewski,[28] M. Woods,[28] G.B. Word,[24] J. Wyss,[21] R.K. Yamamoto,[15]

J.M. Yamartino,[15] X. Yang,[20] J. Yashima,[30] S.J. Yellin,[5] C.C. Young,[28] H. Yuta,[30] G. Zapalac,[33] R.W. Zdarko,[28] and J. Zhou,[20]

[1]*Adelphi University, Garden City, New York 11530*
[2]*INFN Sezione di Bologna, I-40126 Bologna, Italy*
[3]*Boston University, Boston, Massachusetts 02215*
[4]*Brunel University, Uxbridge, Middlesex UB8 3PH, United Kingdom*
[5]*University of California at Santa Barbara, Santa Barbara, California 93106*
[6]*University of California at Santa Cruz, Santa Cruz, California 95064*
[7]*University of Cincinnati, Cincinnati, Ohio 45221*
[8]*Colorado State University, Fort Collins, Colorado 80523*
[9]*University of Colorado, Boulder, Colorado 80309*
[10]*Columbia University, New York, New York 10027*
[11]*INFN Sezione di Ferrara and Università di Ferrara, I-44100 Ferrara, Italy*
[12]*INFN Lab. Nazionali di Frascati, I-00044 Frascati, Italy*
[13]*University of Illinois, Urbana, Illinois 61801*
[14]*E.O. Lawrence Berkeley Laboratory, University of California, Berkeley, California 94720*
[15]*Massachusetts Institute of Technology, Cambridge, Massachusetts 02139*
[16]*University of Massachusetts, Amherst, Massachusetts 01003*
[17]*University of Mississippi, University, Mississippi 38677*
[18]*Moscow State University, Institute of Nuclear Physics 119899 Moscow, Russia*
[19]*Nagoya University, Chikusa-ku, Nagoya 464 Japan*
[20]*University of Oregon, Eugene, Oregon 97403*
[21]*INFN Sezione di Padova and Università di Padova, I-35100 Padova, Italy*
[22]*INFN Sezione di Perugia and Università di Perugia, I-06100 Perugia, Italy*
[23]*INFN Sezione di Pisa and Università di Pisa, I-56100 Pisa, Italy*
[24]*Rutgers University, Piscataway, New Jersey 08855*
[25]*Rutherford Appleton Laboratory, Chilton, Didcot, Oxon OX11 0QX United Kingdom*
[26]*Sogang University, Seoul, Korea*
[27]*Soongsil University, Seoul, Korea 156-743*
[28]*Stanford Linear Accelerator Center, Stanford University, Stanford, California 94309*
[29]*University of Tennessee, Knoxville, Tennessee 37996*
[30]*Tohoku University, Sendai 980 Japan*
[31]*Vanderbilt University, Nashville, Tennessee 37235*
[32]*University of Washington, Seattle, Washington 98195*
[33]*University of Wisconsin, Madison, Wisconsin 53706*
[34]*Yale University, New Haven, Connecticut 06511*
[†]*Deceased*
[a]*Also at the Università di Genova*
[b]*Also at the Università di Perugia*

References

[1] A. Blondel, B. W. Lynn, F. M. Renard, and C. Verzegnassi, Nucl. Phys. **B304**, 438 (1988).

[2] R. D. Field and R. P. Feynman, Nucl. Phys. **B136**, 1 (1978).

[3] R. Brandelik *et al.* (TASSO Collaboration), Phys. Lett. **B100** 357 (1981); C. Berger *et al.* (PLUTO Collaboration), Nucl. Phys. **B214** 189 (1983); W. W. Ash *et al.* (MAC Collaboration), Phys. Rev. Lett. **58** 1080 (1987); T. Greenshaw *et al.* (JADE Collaboration), Z. Phys. **C42** 1 (1989); and D. Stuart *et al.* (AMY Collaboration), Phys. Rev. Lett. **64** 983 (1990).

[4] D. Buskulic *et al.* (ALEPH Collaboration), Phys. Lett. **B335** 99 (1994).

[5] R. Akers *et al.* (OPAL Collaboration), CERN-PPE/95/50 (1995).

[6] P. Abreu *et al.* (DELPHI Collaboration), Z. Phys. **C65**, 569 (1995).

[7] K. Abe *et. al.*, Phys. Rev. Lett. **74**, 2890 (1995).

[8] K. Abe *et. al.*, Phys. Rev. Lett. **74**, 2895 (1995).

[9] K. Abe *et. al.*, Phys. Rev. Lett. **73**, 25 (1994).

[10] M. Hildreth *et al.*, Nucl. Instrum. Methods **A367**, 111 (1995).

[11] G. Agnew *et al.*, Proceedings of the 26-th International Conference on High Energy Physics, pp.1862-1866, Dallas, Texas, August 1992.

[12] E. Farhi, Phys. Rev. Lett **39**, 1587 (1977).

[13] D. Axen *et. al.*, Nucl. Inst. and Meth. **A238**, 472 (1993).

[14] SLD Collab. K. Abe *et al.*, *Phys. Rev.* **D53**, 1023 (1996)

[15] Jets are defined with the JADE algorithm, W. Bartel *et. al.*, Z. Phys. **C33**, 23 (1986), using a value of $y_{min} = 0.02$.

[16] D. Jackson, Nucl. Instrum. Methods **A388**, 247 (1997).

[17] K. Abe *et al.* (SLD Collaboration), SLAC-PUB-7481 (1997), Submitted to Phys. Rev. Lett.

[18] T. Sjöstrand, Computer Phys. Commun. **39** 347, (1986); T. Sjöstrand and M. Bengtsson, Comput. Phys. Commun. **43** 367 (1987).

[19] P.N. Burrows, Stanford Linear Accelerator Center SLD Physics Note 29 (1994) (unpublished).

[20] J.B. Stav and H.A. Olsen, Phys. Rev. **D52**, 1359 (1995); Phys. Rev. **D50**, 6775 (1994).

[21] B. Lampe, Max Planck Institute preprint MPH-PH-93-74 (1993).

[22] A. Djouadi, B. Lampe and P.M. Zerwas, Z. Phys. **C67**, 123 (1995).

[23] D. Buskulic *et al.*, (ALEPH Collaboration), Phys. Lett. **B313**, 545 (1993).